Discover Soil

Research

Spatio-temporal patterns of land use and land cover change in Kibwezi West, Eastern Kenya

Anne Monyenye Omwoyo[1] · Richard Ndemo Onwonga[1] · Oliver Vivian Wasonga[1] · Mwangi James Kinyanjui[2]

Received: 3 August 2024 / Accepted: 4 November 2024
Published online: 25 November 2024

Abstract
Kenyan drylands have over the years undergone extensive land use and land cover (LULC) changes due to population increase, urbanization, agricultural expansion, industrialization and infrastructural developments. There is however limited information on their historical and future spatio-temporal patterns. This study assessed the spatio-temporal LULC change patterns in Kibwezi West for the period 1990–2021 and predicted the LULC map of 2051. Six LULC classes (Forested land, shrubland, grassland, cropland, water body and other lands) covering 1,040.9 Km^2 were examined. Landsat imageries (1990, 2000, 2011 and 2021) were classified using Random Forest algorithm in R software, while LULC change was analyzed using ERDAS Imagine. The 2051 LULC map was predicted using Artificial Neural Network and Cellular Automata algorithms. OpenLand software was used for visualization of LULC patterns using Sankey diagrams. Overall classification accuracy of 78.04% was obtained with 0.61 kappa coefficient. A net loss in forested land (−112.8 km^2), shrubland (−54.48 km^2) and water body (−0.688 km^2) had occurred, with a net gain in cropland (146.03 km^2), grassland (20.24 km^2) and other lands (1.66 km^2) between 1990–2021. Further, a net loss in shrubland (−110.48 km^2), forested land (−89.1 km^2), water body (−0.38 km^2) and other lands (−0.32 km^2) was predicted in 2051 while a net gain was predicted in cropland (176.90 km^2) and grassland (23.39 km^2). The study pointed out historical and future encroachment into natural ecosystems like forested lands and shrublands. The findings of this study contribute to the body of knowledge on LULC dynamics in drylands. These results will inform evidence-based decision-making processes for sustainable land use planning, natural resource management and environmental conservation efforts in Kibwezi West and other similar landscapes.

Keyword Drylands; Sankey diagrams; Sustainable land management; Change detection

1 Introduction

The Earth's land surface is a dynamic combination of different land use and land cover (LULC) types, shaped by natural processes as well as human interventions [1]. However, the ever increasing global population, rapid pace of urbanization, agricultural expansion and industrialization has triggered and driven changes in the composition and configuration of the land surface across the globe [2]. These change drivers could have localized feedback mechanisms on LULC change, and in turn could lead to national, regional or global influences [3]. At the global level, the phenomenon of globalization has significantly influenced LULC patterns [4]. The integration of local economies into the global market has led to increased demand for agricultural products, triggering LULC changes in various regions [5]. These changes span across

✉ Anne Monyenye Omwoyo, omwoyoanne@yahoo.com | [1]Department of Land Resource Management and Agricultural Technology, University of Nairobi, P.O Box 30197, Nairobi 00100, Kenya. [2]Department of Natural Resources, Karatina University, P.O Box 1957, Karatina 10101, Kenya.

different geographical boundaries, therefore impacting ecosystems, biodiversity, and the livelihoods of communities worldwide [6].

Within the African context, land tenure systems have been pivotal in influencing LULC changes. Traditional land management practices and the impacts of colonial era policies have shaped the ownership and utilization of land in many African regions [7, 8]. Historically, drylands of Kenya like Kibwezi West were predominantly subsistence farming and pastoralism [9]. The practices were largely sustainable and in harmony with the local ecology [10]. However, post-colonial land reforms and population pressures have significantly altered this balance [8]. Rapid population growth and urbanization trends in many African countries, including Kenya, have led to increased demand for land for housing, infrastructure, and agriculture [11, 12].

Analysis of LULC change is crucial for understanding the dynamic interactions between human activities and the environment. Understanding the dynamics of LULC change is imperative for various reasons. Firstly, these changes significantly impact the Earth's ecosystems, therefore influencing biodiversity, soil health, and water resources. Secondly, LULC change is complexly linked to climate change, through emission of greenhouse gasses (GHG) and thus influencing regional and global climate patterns [13, 14]. Thirdly, the socio-economic consequences of LULC change are profound, affecting food security, livelihoods, and the resilience of communities in the face of environmental uncertainties [15].

Like other dryland regions, Kibwezi West has experienced significant LULC changes over the past decades [16]. These changes have been driven by a combination of natural factors and human activities, reflecting broader trends observed across the African continent [17, 18]. Kibwezi West is characterized by a semi-arid climate and has traditionally supported a mix of small-scale agriculture and pastoralism. However, recent years have seen shifts towards more intensive agricultural practices, urbanization, and infrastructural development [16]. Deforestation and land degradation are also significant concerns in the area. For instance, the conversion of forested areas to agricultural land has led to loss of biodiversity, alteration of microclimates, and reduced ecosystem services [19–21]. Soil erosion and depletion of soil nutrients are also major issues resulting from unsustainable land use or land management practices in Kibwezi [22].

Past studies have highlighted the impact of LULC change on water resources, soil degradation and biodiversity loss in Kibwezi west [23]. These changes are closely linked to the livelihoods of local communities, affecting agriculture, pastoralism and forestry [10, 24]. A review article by Li, et al. [25] deduced that recent predictive models point towards continued pressure on natural resources in drylands like those in Kibwezi West, due to changes in LULC, raising concerns about long-term sustainability of these areas. These studies call for integrated land management approaches that balance development needs with environmental conservation [25]. Therefore, a comprehensive understanding of the spatio-temporal changes in LULC in these areas will provide crucial information to inform future land management needs that balance social, environmental and environmental factors.

The socio-economic factors influencing LULC changes include population growth, urbanization, and the pursuit for economic development. With the population in Kibwezi and its surrounding areas growing, there has been an increased demand for land for housing, agriculture, and other economic activities [26]. This has led to extensive LULC change through the conversion of natural landscapes into agricultural and urban areas. Understanding these changes is crucial for sustainable land management and conservation strategies in the region [27, 28]. The objectives of this study were to assess the historical spatio-temporal patterns of LULC change (1990 to 2021) and predict future LULC map of the year 2051 for Kibwezi West, in Eastern Kenya. This study contributes to the existing body of knowledge on the past, current and future spatio-temporal trends of LULC change in drylands of Kenya. Additionally, the findings of this study are envisaged to inform policy decisions, community interventions and further academic research on aspects of sustainable land use management practices within Kibwezi West and other similar landscapes.

2 Materials and methods

2.1 Study area

This study was conducted in the lower part of Kibwezi West constituency as shown in * MERGEFORMAT Fig. 1, which covers an area of 1,040.9 Km^2. Kibwezi West is one of the six constituencies in Makueni County, located on the Eastern part of Kenya. Its elevation ranges from 647 to 1993 m above sea level, and is dominated by woody vegetation (shrubs) of different species [16].

According to the Kenyan agroecological zones classification, the study area is semi-arid, falling under the agro-ecological zone V [29]. It lies between latitudes $2^0 5'30''$ S to $2^0 33'0''$ S and longitudes $37^0 40'0''$ E to $38^0 5'0''$ E. The

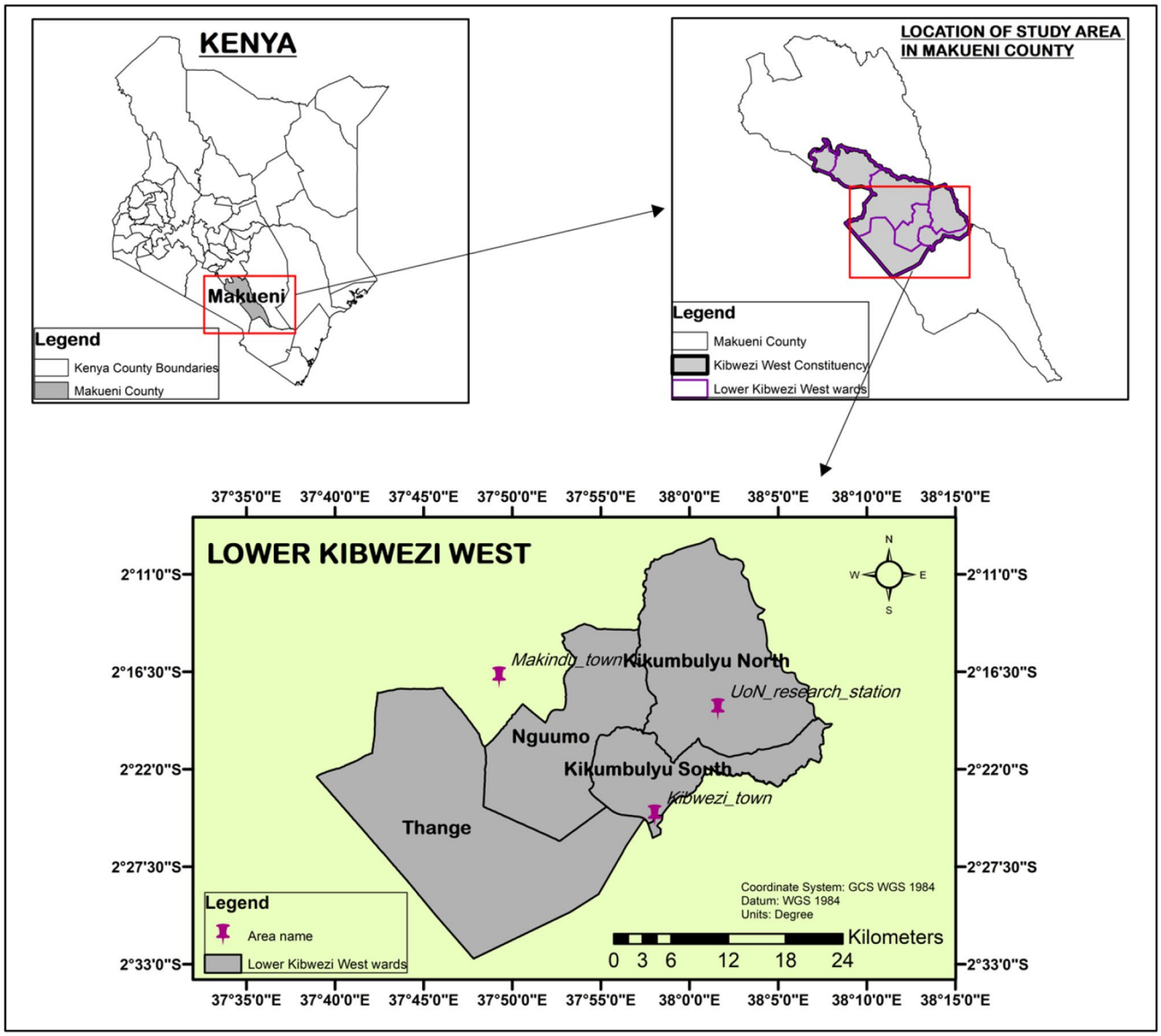

Fig. 1 Map of study area [21]

area receives bimodal rainfall pattern, with unreliable long rains occurring between March and May, and reliable short rains occurring between October and December [30]. The area receives a mean annual rainfall of 600 mm, mean annual minimum temperatures of 14.3 ^{0}C and mean annual maximum temperatures of 35.1 ^{0}C [31]. The dominant soil types, according to the soil classification system of the World Reference Base (WRB IUSS) [32] are Ferralsols and Luvisols.

The inhabitants traditionally earned their livelihood by rearing domestic animals (cattle, sheep and goats), agricultural crop production (green grams, sorghum, millets oranges, cotton, coffee, beans, pigeon peas, sisal, maize, sweet potatoes, mangoes, cassava, tomatoes, and kales). The crop production is mostly done through intercropping and crop rotations [16]. The area has over the years undergone profound LULC changes, therefore leading to land degradation, food insecurity and loss of livelihood [23, 33].

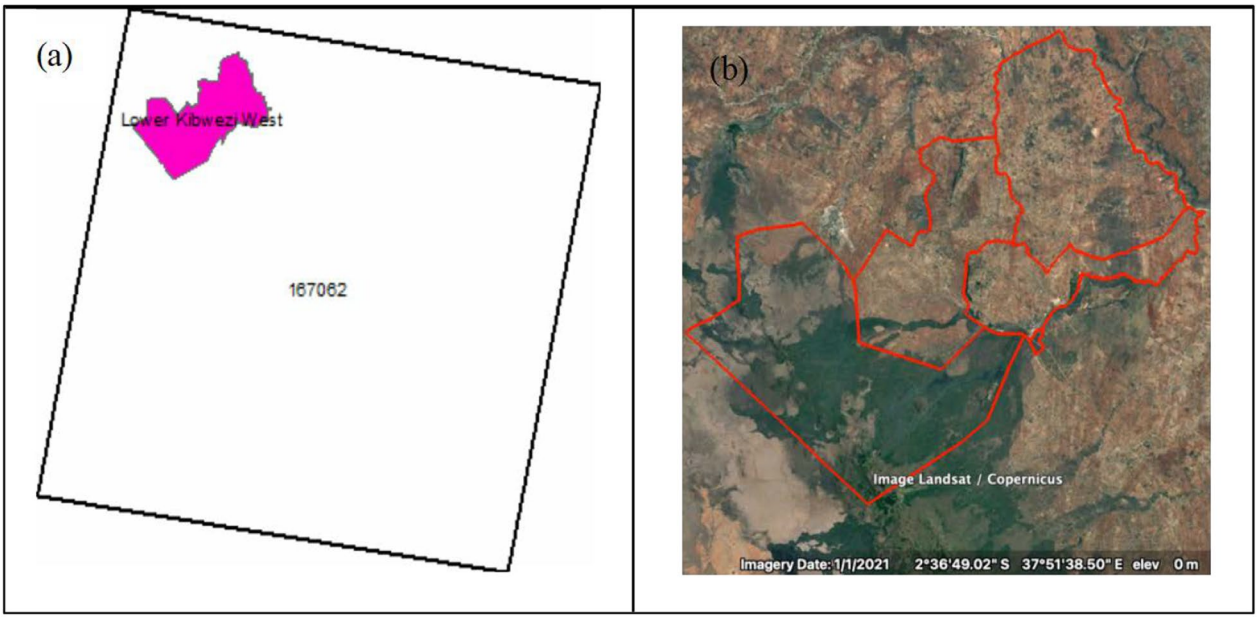

Fig. 2 **a** Raster image (Landsat) scene P167R062 covering the study area and (**b**) satellite image captured in the year 2021 for the study area

Table 1 Description of downloaded Landsat images

Year	Path/Row	Date of acquisition	Satellite	Sensor	Spectral bands	Resolution (Metres)
1990	167/062	02-02-1990	Landsat 5	Thematic Mapper	7	30
2000	167/062	10-02-2000	Landsat 7	Enhanced Thematic Mapper	8	30
2011	167/062	30-02-2011	Landsat 5	Thematic Mapper	7	30
2021	167/062	26-02-2021	Landsat 8	Operational Land Imager (OLI) and Thermal Infrared Sensor	11	30

2.2 Data types and acquisition

Datasets required in analyzing the spatio-temporal patterns of LULC changes were landsat imageries (of a thirty years' period), a digital elevation model (DEM) of 30 m resolution, ground control points (for ground truthing), a map of major roads network and a map of rivers network.The DEM, map of major roads network and map of rivers network were used in future LULC map prediction. A period of thirty years was preferred since the process of change in LULC is slow (depending on the drivers), and a considerable long period of time is recommended for such changes to be detected. Similarly, a projection to the year 2051 was preferred because of the aforementioned reason.

Landsat imageries for the years 1990, 2000, 2011 and 2021 were acquired from the United States Geological Survey (USGS) archive, by generating them using Google Earth Engine (GEE) (https://developers.google.com/earth-engine/datasets/catalog/landsat). GEE is a geo-spatial processing platform used for scientific analysis and visualization of geo-spatial datasets. It hosts current and historical satellite images openly available to the public. A script was set up in GEE for selecting the Landsat image then cloud masking and filtering to the date of interest was done. The process involved setting the parameters for cloud masking the images, setting the time period for the image to be selected from the archives and looping this code for all the years to be downloaded. The cloud cover percentage was limited to 10%. Dry season images (January—March) were selected to avoid any seasonal spectral overlap, then the processed Landsat scene of path 167 and row 062 (P167R062) Fig. 2a), was downloaded for the respective years for further analysis. A satellite image covering the study area was downloaded from Google Earth Pro and presented in Fig. 2b.

A detailed description of the downloaded Landsat images is presented in Table 1. The images were for a 30-year period, in 10-year timesteps. Images for the year 2010 were however not used since they had data gaps, which were

caused by an error due to a failed Scan Line Corrector (SLC) for Landsat 7 ETM [34]. Therefore, the image for the year 2011 was used instead of 2010.

2.3 Preparation of land use and land cover maps

Historical LULC maps for the years 1990, 2000, 2011 and 2021 were developed using the downloaded satellite images based on a supervised classification approach [35] in R software [36]. A ground truthing exercise was carried out to verify signatures identified from classified land cover maps, with what exactly exists on the ground. Accuracy assessment and post-classification was thereafter carried out as explained in Fig. 3 and subsequent sections.

2.3.1 Image preprocessing

Image preprocessing was carried out on the downloaded satellite images to improve the quality of the images and make them suitable for LULC change analysis. The following preprocessing steps were carried out.

2.3.1.1 Geometric correction This step was done to ensure that the images accurately represented the real world and that features in the image were correctly located and measured i.e., ensure spatial accuracy. The satellite images were then transformed and aligned to the common projection of World Geodetic System (WGS) 1984.

2.3.1.2 Cloud and shadow masking This procedure involved removing the effect of cloud and shadow, if any, from the satellite images. Ideally, areas with cloud cover were masked and set to a null value (0). This step was crucial since cloud cover is a major limitation for the use of optical imagery during LULC classification.

2.3.2 Land cover classification

Land cover classification i.e., the process of assigning a land cover class (or class probability) to each image pixel from an image [35], was done using supervised classification through the maximum likelihood method. Supervised classification was preferred since it preserves basic characteristics of LULC due to its statistical technique of classification [37]. The classification categories used for this study (Table 2), were as per what existed in the area, and generally fit the

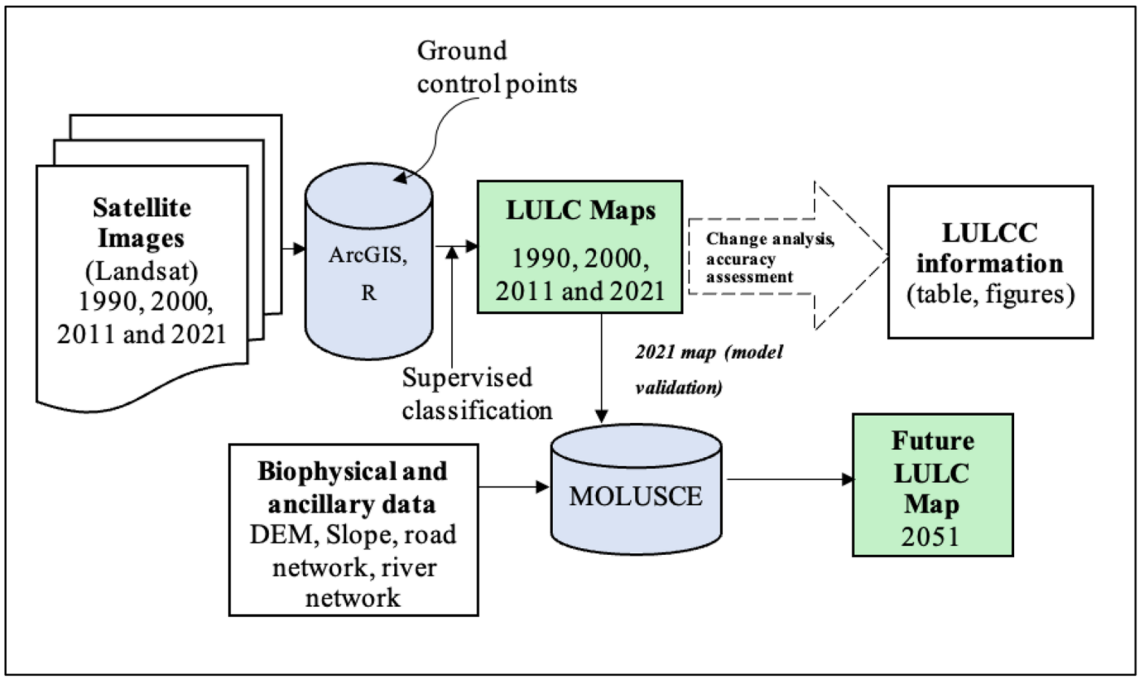

Fig. 3 Methodological flow diagram of the study

Table 2 Definition of the land use and land cover types

LULC type	Description
Forested land	Included all land with woody vegetation consistent with thresholds used to define forested land as defined by FAO [39]. They included gazetted forests (as well as parks and national reserves), forests in private and communal lands
Shrubland	Could also be termed as wooded grassland. It mostly consisted of areas covered in a mix of shrubs, grasses, bare land and trees, with thresholds below (and not anticipated to rise above) those used in the definition of forested land
Grassland	Was composed of treeless grasslands, which were mostly used for pastoralism in the study area and part of the game reserve
Cropland	Land areas purposely managed for agricultural activities, consisting of annual herbaceous crops where crops grow in one or more seasons in a year and at times, such land were bare due to tillage
Water body	Water bodies in the study area and mostly included rivers
Other lands	Developed land, including human settlements, transportation infrastructure, bare soil, rocks and all other un-managed land areas that did not fall into any of the above-mentioned categories

classification system used by the Intergovernmental Panel on Climate Change (IPCC) broad categories (i.e., forest land, grassland, wetland, settlements and other Lands [38].

Random forest (RF) algorithm, which is a supervised classification method was used [40]. The first step was to select training sample sites from the image. The RF was chosen due to its robustness, ability to handle high-dimensional data, and high classification accuracy in remote sensing applications [41]. Training sites were groups of pixels that were identified as having a particular land cover class. They were manually selected and defined as polygons or pixels which were digitized on the image and labeled using a land cover code in ArcGIS, then saved as a shapefile to be used in R software. An already developed R script was used to run the classification. The R script was configured to find; the shapefile for training sites, input image, location of the outputs and margin files. The output product, which was in a tiff format, was color coded, assigned visible colors and thereafter, statistics of each LULC cover category were generated using ERDAS IMAGINE® software as described by Nelson and Khorram [42].

2.3.3 Post classification assessment

Post classification assessment involved validation and accuracy assessment of LULC maps generated. Validation of the first draft of the latest LULC map (2021) was done using ground truth data and high-resolution satellite image for the same year from google earth as an auxiliary data set. Based on the total area of study, a total of 214 points were targeted for validation. A sampling scheme was therefore designed to sample out points for validation purposes based on accessibility (points were generated within 500 m along the roads for easier way of reaching the points) and total area coverage. Stratified random sampling was adopted considering the area proportion of each LULC category against the total area of the study area as shown in Table 3.

Classification accuracy of the generated LULC maps was done by comparing the classification results with ground truth data using the confusion matrix tool. Post-classification refinement was done using the error matrix, which shows the number of pixels that are correctly or incorrectly classified in every land cover class. Following the results of the error matrix, classification was adjusted to improve accuracy. Accuracy assessment was determined using the error matrix, Kappa coefficient, producer accuracy and consumer accuracy as described by Rwanga and Ndambuki [43].

Table 3 Sampling points for validation of LULC categories

LULC category	Number of points to be validated
Forested land	7
Shrubland	92
Grassland	2
Cropland	104
Settlement/other lands	7
Water body	2
Total	214

2.4 Population projection

Projection of population for the study area was necessary since the information would help in interpretation of the predicted LULC map. Population data was analyzed for the years 1999, 2009, and 2019 based on the sub-location administrative units and as obtained from the Kenya Bureau of Statistics (KNBS) in line with national census. Using this population data, an interpolation was done for the year 2051 using linear regression at 95% confidence interval, in the FORECAST function of excel as further described in Wilson [44].

2.5 Prediction of future land use and land cover map

2.5.1 Selection of explanatory variables

Explanatory variables were defined as those variables that would have the capability of contributing to the changes in future LULC patterns. The explanatory variables chosen for this study were elevation, slope, distance from roads, distance from rivers and population projection. Elevation and slope were derived from the DEM in ArcGIS using the spatial analyst tool. Distance from roads and distance from rivers were calculated using the Euclidean method in ArcGIS from major roads and rivers network vector layers respectively. The significance of the spatial variables in predicting future LULC change was tested using the Cramer's coefficient (Cramer's V) in Modules for Land Use Change Evaluation (MOLUSCE) plug-in running in QGIS v2.16.3. Cramer's V shows the association between two variables, and in this case, between the spatial variables and LULC [45].

2.5.2 Transition potential modeling

Prediction of future LULC was done using the MOLUSCE plug-in running in QGIS v2.16.3 as described in Hakim, et al. [46]. The plug-in incorporates well known algorithms that can be used in the analyses of LULC change, forestry and urban projects. MOLUSCE was used to estimate the spatio-temporal changes and transitions in LULC between 1990 – 2000, 2000 – 2011 and 2011 – 2021. The artificial neural network (ANN) and Monte Carlo cellular automata (CA) algorithms within MOLUSCE were used to evaluate LULC transition potentials and to simulate/predict future LULC map for 2051 for the study area. The CA-ANN algorithm simulates LULC change using a raster-based grid system with transition probabilities to simulate change over time as described by Al-Hameedi, et al. [47]. CA-ANN has been widely used and is documented to be effective as compared to linear regression [48]. For the prediction, a minimum of 1,000 iterations, a neighbourhood value of one pixel, a learning rate of 0.1, 10 hidden layers and momentum value of 0.05 were set in the ANN model.

2.5.3 Validation of the model

In conjunction with the LULC maps for 1990 and 2011, transition potential matrices and the explanatory spatial variables (mentioned in Sect. 2.5.1) were used to predict the LULC map for 2021. In order to validate the model and predict outcome's accuracy, the technique of kappa validation (standard kappa, kappa histogram and kappa location) was used to compare the predicted 2021 map vis-a-vis the actual 2021 map (which was classified). Three model validation iterations were run in CA-ANN. After successful validation of the model, LULC the initial LULC map (1990) and the final LULC map (2021), together with the explanatory spatial variables, were used in predicting LULC map for 2051.

2.6 Land use and land cover change analysis

Image differencing was used to determine LULC change extent (Eq. 1), whereby results of gains, losses, net change or persistence in LULC change categories was presented in the form of maps, diagrams, graphs and tables. Sankey diagrams of LULC dynamics, transition matrices as well as gross and net changes in LULC types over the years were drawn using R software's Open-land and NetworkD3 package as described by [49]. The percent change and annual rate of change in LULC were calculated following Leta, et al. [50], using equations Eq. 2 and Eq. 3 respectively.

$$Change\,(Km^2) = A_f - A_i \tag{1}$$

$$Percent\ change\ (\%) = \frac{A_f - A_i}{A_i} * 100 \quad (2)$$

$$Rate\ of\ change\ (Km^2/year) = \frac{A_f - A_i}{T} \quad (3)$$

where A_f is the area of later LULC map (Km^2), A_i is the area of initial LULC map (Km^2) and T is the time interval (number of years) between A_f and A_i (years).

3 Results

3.1 Classification accuracy

An overall classification accuracy of 78.04% and a Kappa Coefficient of 0.61 was obtained, whereby 167 points out of the 214 sampled for validation were classified accurately (Table 4). Such classification accuracy is considered satisfactory for heterogeneous management practices using medium resolution satellite imageries [51]. A categorization of widely referenced Kappa statistic values is presented in Rwanga and Ndambuki [43], where values of Kappa coefficient ranging 0.61 to 0.80 are rated as substantial and thus the generated LULC maps were fit for further analysis.

3.2 Spatio-temporal land use and land cover classification

Image classification results for the years 1990, 2000, 2011 and 2021 are presented in Fig. 4. Area coverage of the different LULC types under study is also presented in Fig. 5. Shrubland dominated the study area from the year 1990 to 2021, covering between 41.6% (433 km^2) to 52.9% (550.94 km^2) of the total area (Fig. 5). Its coverage however reduced in the year 2000 by transitioning to the other LULC types. Forested land was the second dominant land cover class in 1990, covering 266.10 km^2 which corresponds to 25.57% of the total land area. Its coverage increased in the year 2000, but later decreased through the years 2011 and 2021. By the year 2021, the second dominant LULC type was cropland which covered 33.5% (348.6 Km^2) (Fig. 5). Forested land, grassland, water body and other lands covered 14.7% (153.2 Km^2), 3.8% (39.6 Km^2), 0.1% (1.1 Km^2) and 0.2% (1.9 Km^2) respectively.

3.3 Historical land use and land cover change statistics

Historical land use and land cover change statistics are presented as percent changes and annual rates of change. Between the years 1990 –2000, a decrease in area coverage was found to have occurred in cropland, water body and shrubland at –13%, –9.7% and –8.8% respectively (Table 5). The rate of decrease was high in shrubland (–4.8 Km^2/year), followed by cropland (–2.6 Km^2/year) then water body (–0.02 Km^2/year). On the contrary, grassland, forested land and other lands were found to have increased by 169.1%, 15.3% and 810.0% respectively. The rate of increase was however high in forested land (4.1 Km^2/year) as compared to grassland (3.3 Km^2/year) and other lands (0.16 Km^2/year) (Table 5).

Table 4 Error (confusion) matrix of LULC classification

LULC Class	C	FL	G	WB	O	SL	Total	Producer Accuracy	User Accuracy
C	89	0	0	0	1	25	115	86%	77%
FL	0	5	0	0	0	1	6	71%	83%
G	1	0	2	0	0	1	4	100%	50%
WB	0	0	0	2	0	0	2	100%	100%
O	0	0	0	0	4	0	4	57%	100%
SL	14	2	0	0	2	65	83	71%	78.3%
Validated Totals	104	7	2	2	7	92	214		

C cropland, *FL* Forested land, *G* grassland, *WB* Water body, *O* Other lands, *SL* shrubland

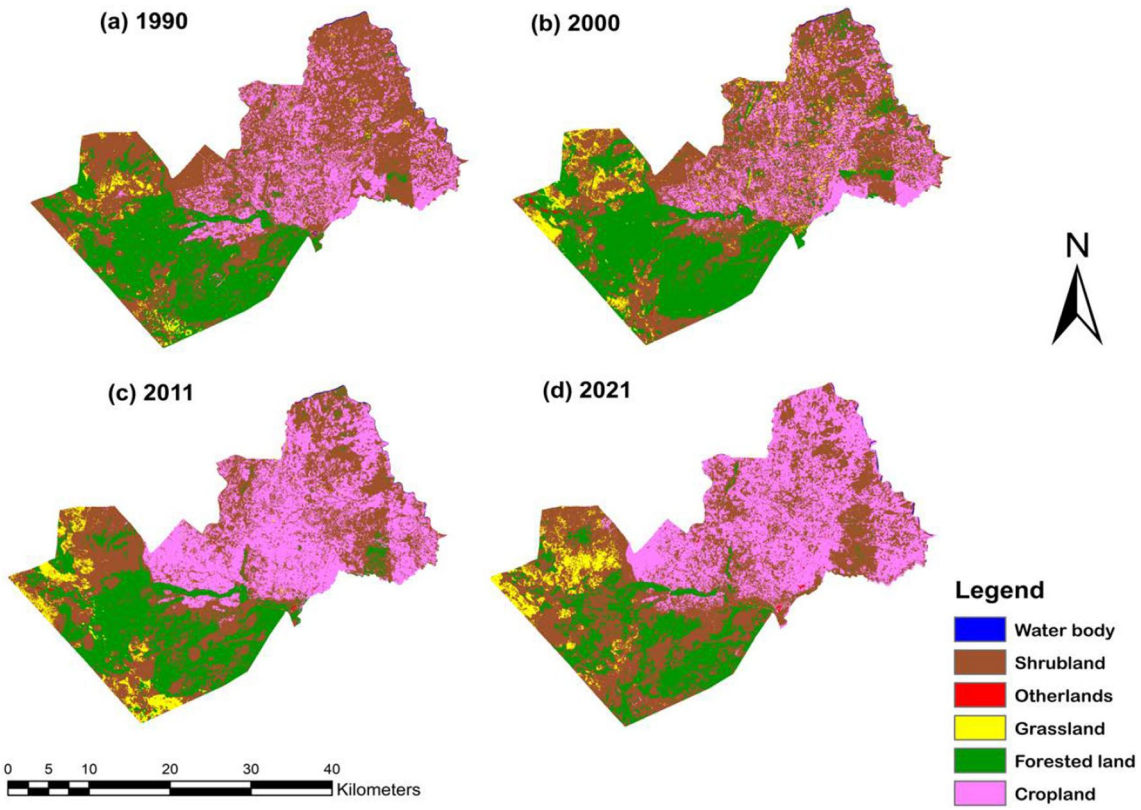

Fig. 4 Classified land use and land cover maps for the study area in the years (**a**) 1990, (**b**) 2000, (**c**) 2011 and (**d**) 2021

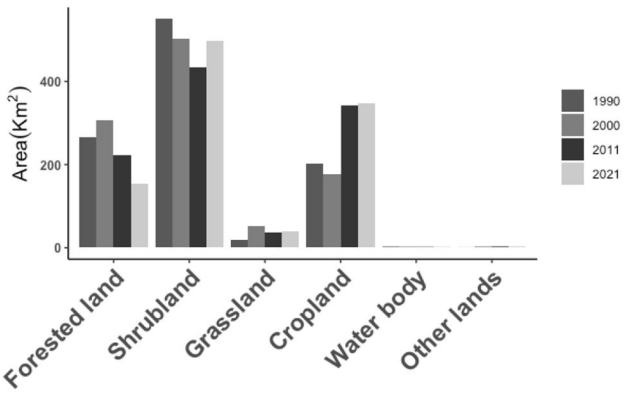

Fig. 5 Area coverage of different LULC types in the study area between the years 1990, 2000, 2011 and 2021

Table 5 Percent change and annual rate of change in land use and land cover between 1990 and 2021

LULC	Percent change (%) in LULC			Rate of change (Km2/year) in LULC		
	1990–2000	2000–2011	2011–2021	1990–2000	2000–2011	2011–2021
FL	15.3	−27.0	−31.6	4.1	−7.5	−7.1
SL	−8.8	−13.9	14.7	−4.8	−6.3	6.3
G	169.1	−26.9	4.1	3.3	−1.3	0.2
C	−13.0	94.7	1.6	−2.6	15.2	0.6
WB	−9.7	−33.6	6.1	−0.02	−0.05	0.01
O	810.0	7.1	−4.6	0.16	0.01	−0.01

FL Forested land, *SL* shrubland, *G* grassland, *C* cropland, *WB* Water body, *O* Other lands

In 2000–2011, a decrease in area coverage occurred in forested land, shrubland, grassland and water bodies at −27%, −13.9%, −26.9% and −33.6% respectively (Table 5). The rate of decrease was high in forested land (−7.5 Km^2/year) and low in water body (−0.05 Km^2/year). On the contrary, cropland and other lands were found to have increased by 94.7%, 7.1% respectively. The rate of increase was high in cropland (15.2 Km^2/year) and low in other lands (0.01 Km^2/year) (Table 5).

Between 2011 and 2021, there was a decrease in area coverage in forested land and other lands at −31.6% and −4.6% respectively (Table 5). The rate of decrease was high in forested land (−7.1 Km^2/year) and low in other lands (−0.01 Km^2/year). On the contrary, shrubland, grassland, water body and cropland were found to have increased by 14.7%, 4.1%, 6.1% and 1.6% respectively. The rate of increase was however high in shrubland (6.3 Km^2/year) and low in water body (0.01 Km^2/year) (Table 5).

3.4 Prediction of land use and land cover map for 2051

3.4.1 Spatial variables for prediction of land use and land cover change

The explanatory spatial variables (elevation, slope, distance from roads, distance from rivers) used for this study are presented in Fig. 6. Their significance was evaluated in the MOLUSCE plugin in QGIS using Cramer's value. Cramer's values range from zero (0) to one (1) with one representing a strong association between LULC and the spatial variables. A value of 0 represents no association between the spatial variables and LULC patterns. The Cramer's value for the spatial

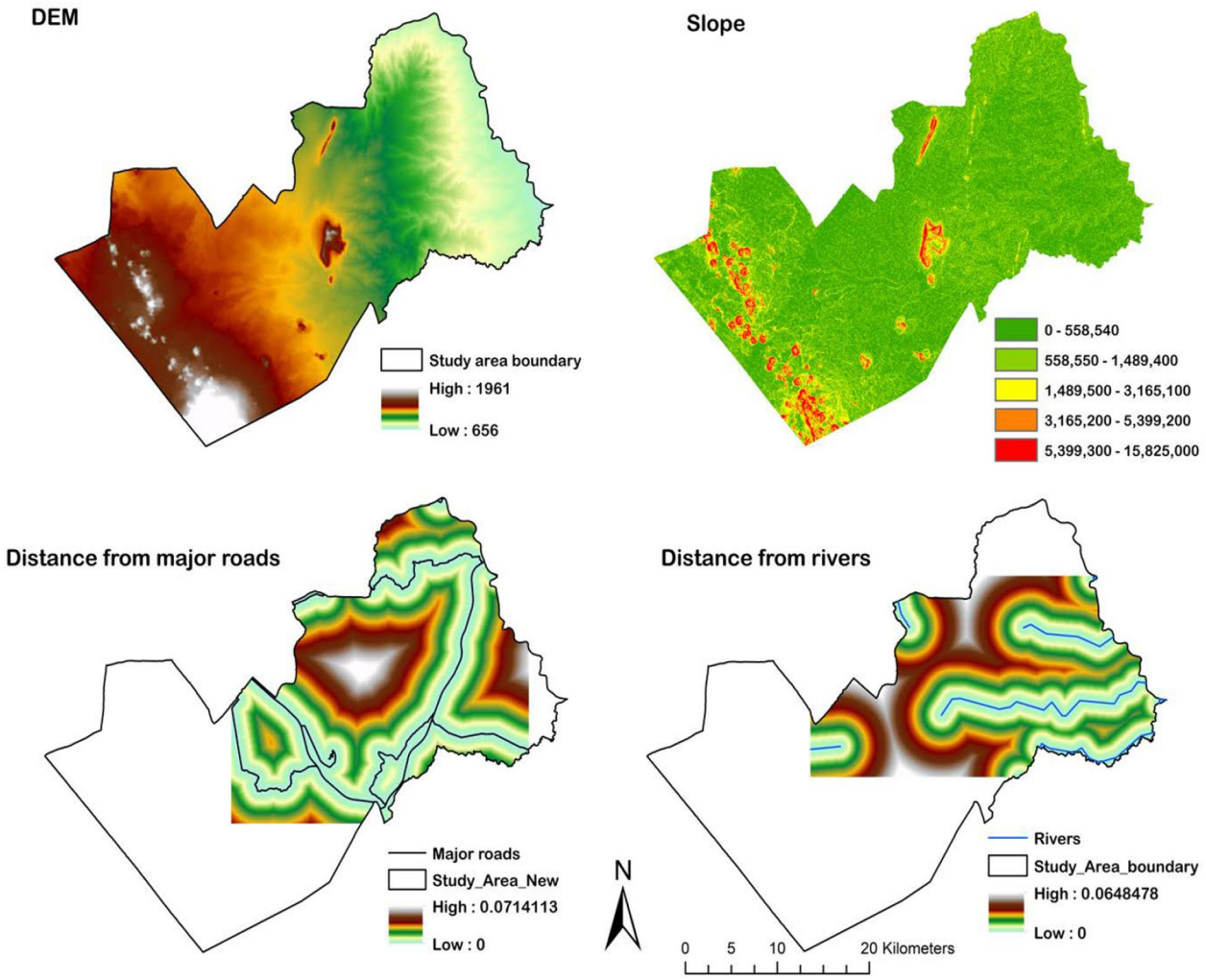

Fig. 6 Spatial layers used for predicting future LULC map

variables in this study is indicated in Table 6. Cramer's V of ≥ 0.15 are usually considered substantial and therefore the variables should be considered in modeling [45, 46].

3.4.2 Population projection

Population projection in the study area was found to have an increasing trend over the years. The population was projected to increase by 47% from 143,786 people in 2019 to 211,531 people in 2051 (Table 7). The upper and lower confidence bounds are also indicated in Table 7.

3.5 Model validation

In MOLUSCE, model validation was done by comparing the predicted map of the year 2021 and the actual map of the year 2021. After several model iterations, and thereafter comparing the predicted LULC map of 2021 and the actual LULC map of the same year, satisfactory statistics were acquired. The kappa statistics for predicted maps of 2021 and 2051 are presented in Table 8. During the model learning process, the minimum validation overall error was 0.01512 and 0.02117 for 2021 and 2051 respectively.

3.6 Predicted land use and land cover map for the year 2051

The predicted LULC map of the year 2051, in comparison to the LULC map of 2021 is presented in Fig. 7. Area coverage of the different predicted LULC types is also presented in Fig. 8. From the prediction, it was anticipated that cropland would dominate the study area by covering 50.5% (525.5 km^2) of the total area by the year 2051 (Fig. 8). Shrubland would be the second dominant LULC type, covering 37.1% (386.0 km^2) of the total land area. Forested land, grassland, other lands and water body were predicted to cover 6.2% (64.1 Km^2), 6.1% (63.0 Km^2), 0.2% (1.5 Km^2) and 0.1% (1.7 Km^2) respectively (Fig. 8).

Table 6 Cramer's coefficient values of the spatial variables

Spatial variable	Cramer's coefficient
Digital elevation model (DEM)	0.39
Slope	0.31
Distance from major roads	0.19
Distance from rivers	0.16

Table 7 Population projection in the study area

Year	Population	Forecast	Lower confidence bound	Upper confidence bound
1999	94,627	–	–	–
2009	94,003	–	–	–
2019	143,786	143,786	143,786	143,786
2029	–	161,853	132,774	190,932
2039	–	184,434	154,784	214,083
2049	–	207,015	176,125	237,904
2051	–	211,531	180,213	242,849

Table 8 Kappa values for predicted maps of the years 2021 and 2051

	2021	**2051**
Percent correctness	93.75	88.10
Kappa (overall)	0.90	0.80
Kappa (histogram)	0.92	0.96
Kappa (location)	0.98	0.84

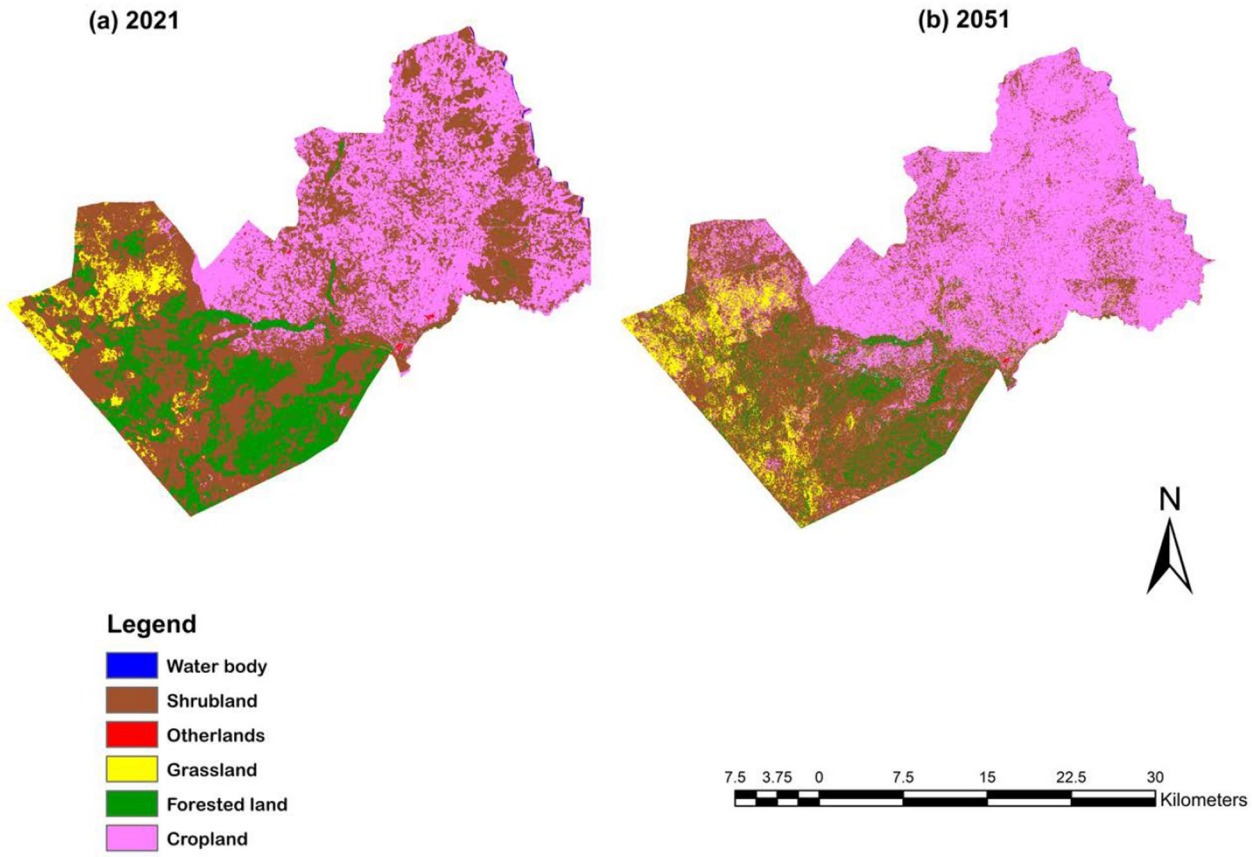

Fig. 7 Classified LULC map of 2021 (**a**) and predicted LULC map of 2051 (**b**)

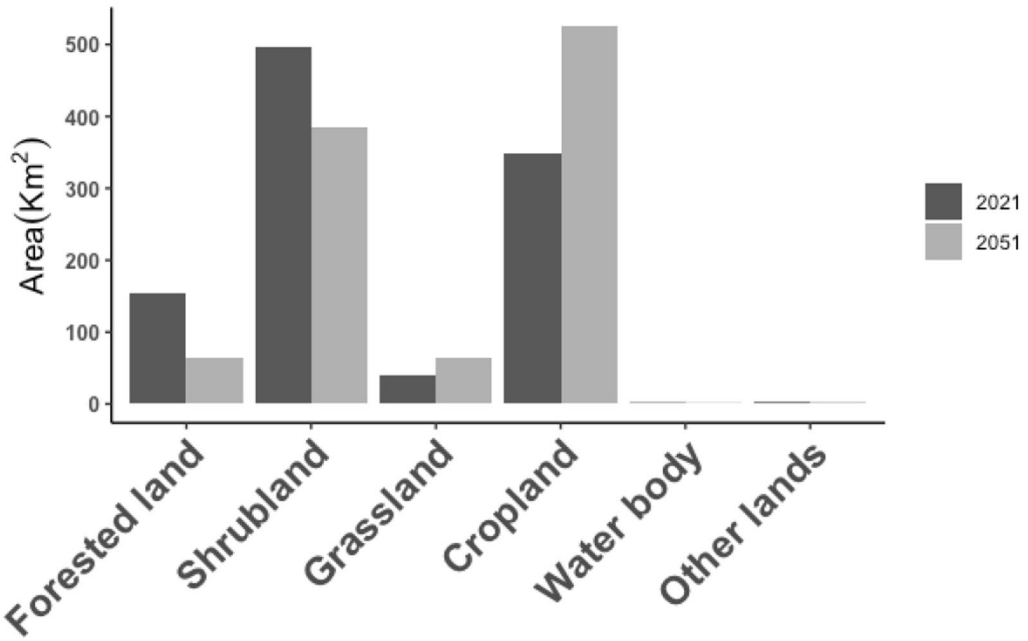

Fig. 8 Area coverage of different LULC types in Kibwezi West between the years 2021 and 2051

Table 9 Percent change and annual rate of change in land use and land cover between 2021 and 2051

LULC	Percent change (%) in LULC 2021—2051	Rate of change (Km2/year) in LULC 2021—2051
FL	−58.9	−3.0
SL	−22.3	−3.7
G	59.1	0.8
C	50.7	5.9
WB	−37.1	−0.01
O	−17.7	−0.01

FL Forested land, *SL* shrubland, *G* grassland, *C* cropland, *WB* Water body, *O* Other lands

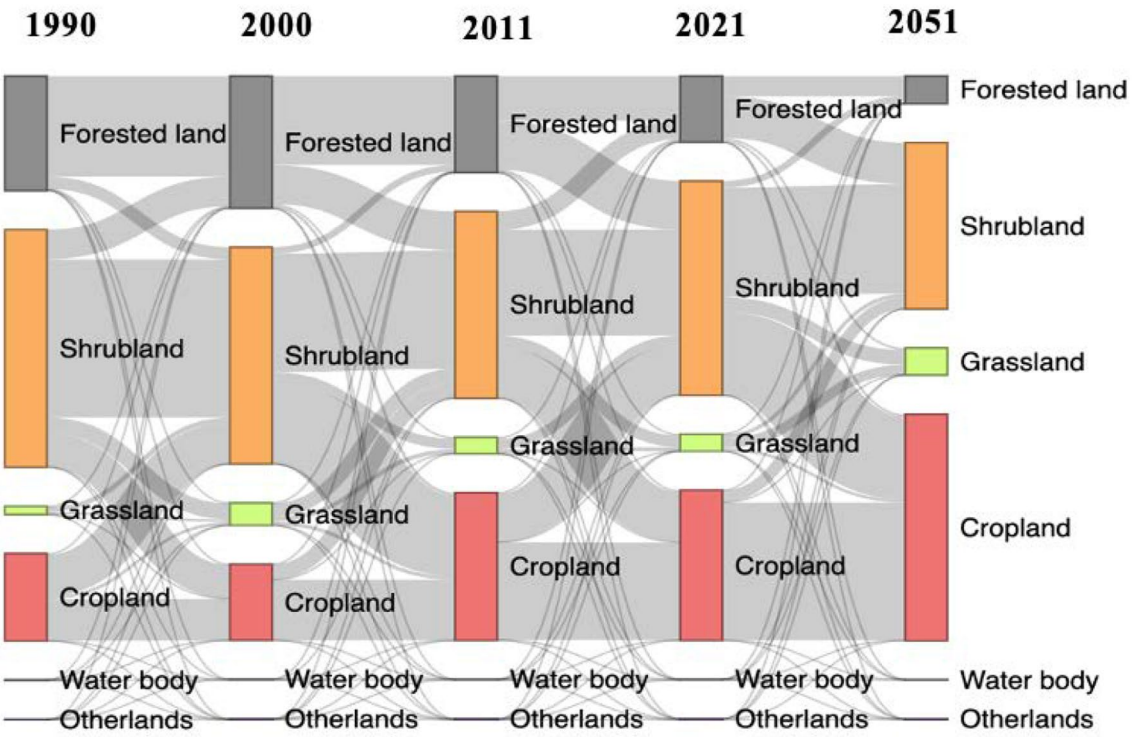

Fig. 9 Sankey diagram for comparison of land cover dynamics in four land cover maps for the years 1990, 2000, 2011, 2021 and 2051. The lines (paths) show transition of LULC classes in the study area between the years

3.7 Predicted land use and land cover change statistics

Between the years 2021 to 2051, there was an increase in area coverage under cropland and grassland at 59.1% and 50.7% respectively. The rate of increase was however higher in cropland (5.9 Km^2/year) than in grassland (0.8 Km^2/year). On the contrary, forested land, shrubland, water body and other lands decreased by 58.9%, 22.3%, 37.1% and 17.7% respectively. The rate of decrease was however high in shrubland (3.7 Km^2/year) and low in water body (0.01 Km^2/year) (Table 9).

3.8 Land use and land cover change dynamics between 1990 to 2051

The Sankey diagram (Fig. 9) visualizes LULC extent and dynamics in the study area between the years 1990, 2000, 2011, 2021 and 2051. It is accompanied by a cross-tabulation (transition area matrices) between these years (Table 10

Table 10 Transition area matrix for land use and land cover change between the years 1990–2021

1990 – 2000 area transformations (%)		FL	SL	G	C	WB	O	Total
	FL	22.42	2.74	0.15	0.14	0.00	0.11	**25.57**
	SL	6.62	35.19	3.53	7.50	0.06	0.04	**52.93**
	G	0.12	1.10	0.57	0.07	0.00	0.00	**1.86**
	C	0.31	9.22	0.72	9.21	0.01	0.00	**19.46**
	WB	0.01	0.04	0.02	0.01	0.07	0.01	**0.16**
	O	0.00	0.00	0.00	0.00	0.00	0.01	**0.02**
	Total	**29.47**	**48.29**	**5.00**	**16.93**	**0.14**	**0.17**	**100.00**
2000 – 2011 area transformations (%)		**FL**	**SL**	**G**	**C**	**WB**	**O**	**Total**
	FL	19.80	8.70	0.33	0.61	0.00	0.03	**29.47**
	SL	1.50	26.37	2.31	18.03	0.02	0.07	**48.29**
	OG	0.11	3.04	0.99	0.83	0.01	0.03	**5.00**
	C	0.05	3.38	0.04	13.45	0.00	0.01	**16.93**
	WB	0.01	0.04	0.00	0.03	0.06	0.00	**0.14**
	O	0.04	0.07	0.00	0.01	0.01	0.05	**0.17**
	Total	**21.51**	**41.60**	**3.65**	**32.95**	**0.09**	**0.19**	**100.00**
2011 – 2021 area transformations (%)		**FL**	**SL**	**G**	**C**	**WB**	**O**	**Total**
	FL	9.96	10.85	0.30	0.38	0.01	0.01	**21.51**
	SL	4.12	23.60	2.62	11.15	0.04	0.07	**41.60**
	G	0.37	2.30	0.86	0.13	0.00	0.00	**3.65**
	C	0.23	10.83	0.02	21.74	0.04	0.09	**32.95**
	WB	0.00	0.03	0.00	0.05	0.01	0.00	**0.09**
	O	0.04	0.09	0.01	0.04	0.01	0.01	**0.19**
	Total	**14.72**	**47.70**	**3.80**	**33.49**	**0.10**	**0.18**	**100.00**

Table 10 (continued)

FL Forested land, *SL* shrubland, *G* grassland, *C* cropland, *WB* water body, *O* other lands, shaded box = percentage of no transition

Table 11 Transition area matrix for land use and land cover change between the years 2021–2051

2021 – 2051 area transformations (%)		FL	SL	G	C	WB	O	Total
	FL	4.50	9.24	0.49	0.49	0.00	0.01	**14.72**
	SL	1.50	24.38	3.26	18.53	0.01	0.03	**47.70**
	G	0.04	0.84	2.23	0.69	0.00	0.00	**3.80**
	C	0.11	2.58	0.08	30.67	0.01	0.04	**33.49**
	WB	0.00	0.01	0.00	0.04	0.04	0.00	**0.10**
	O	0.01	0.03	0.00	0.09	0.00	0.06	**0.18**
	Total	**6.16**	**37.09**	**6.05**	**50.49**	**0.06**	**0.15**	**100.00**

FL Forested land, *SL* shrubland, *G* grassland, *C* cropland, *WB* water body, *O* Other lands, shaded box = percentage of no transition

and Table 11), which indicate the persistence and transitions during the time intervals of 1990–2000, 20–2011, 2011–2021 and 2021–2051. The height of bars in each column of Fig. 9 represent abundance of the land use classes in the study area at a particular year. In the last three decades, major gross transitions were amongst forested land, shrubland, cropland and grassland as indicated by the thickness of paths in Fig. 9. Forested land was mostly lost to shrubland, with a peak transition of 10.85% occurring in 2011–2021 (Table 10). Shrubland majorly lost its coverage area to grassland, cropland and forested land, with a high transition occurring between 2000 and 2011, whereby 18.03% of shrubland transitioned to cropland (Table 10). In cropland, most of its area coverage was lost to shrubland, with a high transition area of 10.83% being experienced between 2011 and 2021. The coverage area for grassland was majorly lost to shrubland, with a high transition of 3.04% being experienced during 2000–2011 (Table 10). By the year 2051, forested land was predicted to lose 9.24% of its area coverage to shrubland while 18.53% of shrubland would be lost to cropland (Table 11). Transitions in the remaining LULC types were below 1% (Table 11).

3.9 Net gains and net losses in land use and land cover

Net gains and net losses in area coverage of different land use and land cover classes between the years 1990 and 2021 is presented in Fig. 10. Forested land, shrubland and water body were found to experience a net loss of coverage area between the years 1990 to 2021 (Fig. 10). Highest net loss of −12.86 km^2 was experienced in forested land while the lowest net loss of -0.68 km^2 was experienced in the water body. Shrubland had an intermediate net loss of -54.48 km^2 in its area. In contrast, cropland, grassland and other lands had a net gain of coverage area between the years 1990 to 2021 (Fig. 10). Highest net gain of 146.03 km^2 was found to have been experienced in cropland, while the lowest net gain of 1.66 km^2 was experienced in other lands. Grasslands had an intermediate net gain of 20.24 km^2.

Net gains and net losses in area coverage of different land use and land cover classes between the years 2021 and 2051 are presented in Fig. 11. From the results, an indication of possible net loss in coverage area for forested land, shrubland, water body and other lands was predicted between the years 2021 to 2051 (Fig. 11). Highest net loss of -110.48 km^2 was predicted to occur in shrublands while lowest net loss of -0.32 km^2 was in other lands.

Forested land and water body were found to have intermediate coverage area net losses of -89.10 km^2 and -0.38 km^2 respectively. On the contrary, grassland and cropland were predicted to experience net gains in their coverage areas

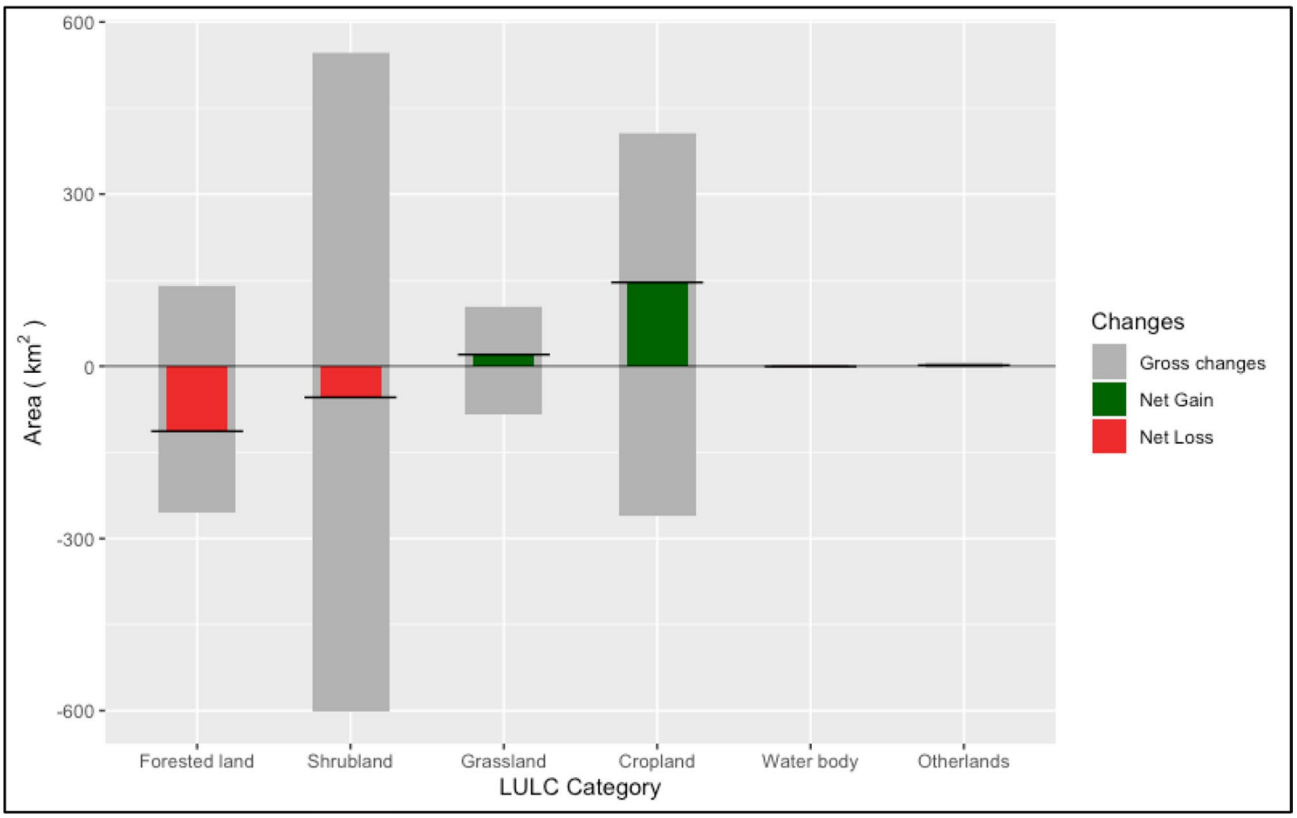

Fig. 10 Comparison of overall changes in LULC types between the years 1990 to 2021

between the years 2021 and 2051. Cropland would have the highest net gain of 176.90 km^2 while grasslands would have the lowest net gain of 23.39 km^2 (Fig. 11).

4 Discussion

4.1 Image classification and accuracy

Satisfactory classification accuracy and Kappa Coefficient from this study demonstrates reliable and credible analysis. Rwanga and Ndambuki [43] state that Kappa coefficients of 0.61 to 0.80 have a substantial rate of agreement in assessing classification accuracy. Comparatively, due to varying factors like classification algorithms, complexity of landscapes and imagery resolution, similar studies in drylands reported varying classification accuracies. Nouri, et al. [52] for instance, reported accuracies ranging between 70 and 85% when they classified a semi-arid region of Iran using images of medium resolution. Additionally, Oduke, et al. [53] reported overall classification accuracy of 81% for a LULC change analysis in Kitui Kenya, which is a comparable environment to Kibwezi West. However, discrepancies were realized while comparing this study's accuracy levels to those that used images of higher resolution. For instance, the work by Chapa, et al. [54], reported classification accuracies of over 85% using higher resolution images. This difference could be attributed to the varied spatial resolution, as medium-resolution satellite imagery tends to struggle with capturing fine-scale details in heterogeneous environments, a limitation that has been highlighted in other studies [55].

4.2 Population projection

A population projection of 47% increase from 2019 to 2051 (Table 7) is a critical factor when it comes to influencing LULC transitions. The growth is expected to exert pressure on resources like land, therefore leading to increased conversion of natural ecosystems because of increased demand for agricultural land, settlement areas and infrastructure. Such

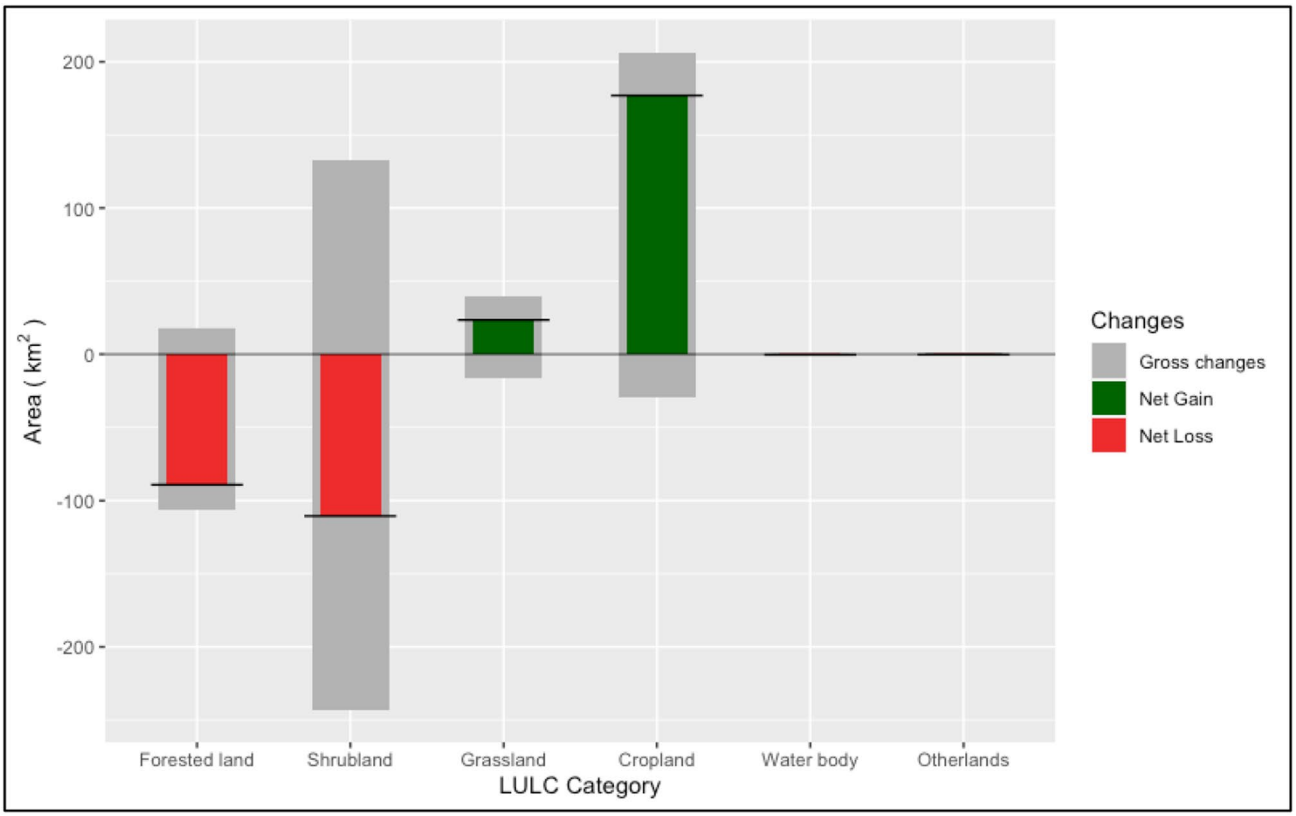

Fig. 11 Comparison of overall changes in LULC classes between the years 2021 and 2051

demographic pressures have been documented as drivers of LULC change, as noted by Güneralp, et al. [56] in their study of forecasting urban expansion and their impacts on biodiversity and carbon pools.

4.3 Land use land cover classification and change detection

Despite the water (moisture) stress and poor soils in drylands of Kenya like those in Kibwezi West, these ecosystems play a crucial role in environmental sustainability and supporting livelihoods of the people who live there. Unfortunately, as presented in the findings of this research, extensive LULC change was reported to have been experienced over the last three decades in Kibwezi west. The historical analysis revealed noteworthy shifts in LULC patterns between 1990 and 2021. The dominance of shrubland and cropland in the study area highlighted the agricultural and natural landscape characteristics of the region. However, the observed decrease in forestland and water bodies points towards the environmental changes and potential ecological impacts of anthropogenic activities. Such trends could possibly lead to a reduction in soil organic carbon and increased greenhouse gas emissions to the atmosphere as pointed out by Omwoyo, et al. [21].

The observed increase in coverage area under shrubland was at the expense of forested land, since a larger proportion of forested land was observed to have transitioned to shrubland. This can be related to increased forest encroachment from nearby communities as well as infrastructure development projects like the standard gauge railway (SGR), whereby portions of Kibwezi Forest were cleared to pave way for construction of the railway. Similar findings were reported by Sang, et al. [57], whereby their study found out that construction of the SGR led to immense LULC change along its corridor. Additionally, the loss in forest cover that was observed between 2000 and 2011 could be because of the increase in settlements/other lands that was observed between 1990 – 2000. The demand for land for settlement and other infrastructural developments could have put pressure on the natural ecosystems like forested lands, shrublands and grasslands. These findings are in line with those of Mugambi, et al. [23], who reported that high levels of deforestation were experienced in Kenya's forested areas between the years 2000–2010 through search of firewood, other forest products and farming. Residents of Kibwezi West traditionally practice subsistence farming and rear animals that require grazing, and therefore this could explain the predicted increase in coverage area of grasslands by the year 2051.

Other reasons for the decline in area coverage of forested land could be attributed to forest fires either naturally occurring or because of prolonged dry spells. A report by the GoK [58] indicated that most forest fires in Eastern Kenya occurred between the years 2000 and 2010. Under cropland, the observed increase in its coverage area was at the expense of other LULC types, majorly shrublands, and this depicted an expansion in food production. The reason behind this could be because of increased demand for subsistence and commercial agricultural produce, due to increased population as was observed in the study area. These observations are in agreement with those of Ruttoh, et al. [16] who reported that there was a great conversion of the natural vegetation into agricultural lands and built up areas.

Consequently, a decline in the natural ecosystems (forested areas, shrublands and grasslands) that was observed between 2000 and 2011 could have led to the reduction in water bodies. The natural ecosystems are key catchment areas to streams and rivers, hence their destruction led to reduced water discharge. Similar findings were presented in Mwaura, et al. [59], whereby over the same period, some of Kibwezi's permanent rivers had dried up while others had turned to be seasonal due to human interference through LULC change. Other studies, like those of Omwoyo, et al. [60] found similar trends of reduced stream flow due to catchment degradation. Further, similar concerns about the loss of natural vegetation and its impact on ecosystem services have been raised by recent studies in other drylands, such as that by Tesfay, et al. [61], who noted that the degradation of shrublands in Ethiopia led to increased vulnerability to climate change.

Further, the observed high percentage of expansion in other lands (a LULC type which included settlement areas) between 1990 and 2000 could be attributed to encroachment and in-migration of people to Kibwezi in search of land to settle. The government of Kenya introduced the 'Shamba System' in the late 1990's and early 2000's for people to intercrop annual crops with targeted indigenous tree seedlings in forested areas. The system however failed, leading to encroachment and degradation of forests [62].

4.4 Land use and land cover change transitions

The transition pathways depicted in the Sankey diagrams visually represent the conversion of LULC types, illustrating the complex interactions and transformations occurring within the landscape. The net gains and losses analysis revealed contrasting trends among different LULC types. This, therefore, reflected the dynamic nature of land use practices, which can include deforestation, agricultural expansion, and urban development. All these factors have significant implications for ecosystem services, biodiversity, and land degradation in Kibwezi West.

Looking ahead to the projected scenarios for 2051, the anticipated increase in cropland and grassland areas suggests continued intensification of agricultural activities and potential land use diversification. However, the anticipated net losses in forested land, shrubland, water bodies, and other lands suggest potential challenges in biodiversity conservation, ecosystem resilience, and sustainable land management in the future. These results mirror the trends observed in other regions of Africa, where agricultural land expansion was forecasted to be driven by population growth and the need for increased food production [63, 64]. The projected population increase in the study area by 47% between 2019 and 2051 reinforces this prediction, as previous studies have demonstrated strong correlations between population growth and agricultural land expansion in dryland regions [65]. Similar population–driven LULC dynamics were reported by Assede, et al. [17], who linked demographic pressures to significant land cover changes in Africa. However, the predicted decline in forested land (−58.9%) by 2051 raises concerns about the sustainability of land use practices, especially given the essential ecosystem services provided by forests in terms of carbon sequestration and biodiversity conservation.

Overall, the findings of this research provide valuable insights for land use planning, conservation strategies, and sustainable development initiatives in the Kibwezi West region. This study has demonstrated the importance of monitoring LULC patterns and dynamics. The results can be used to promote sustainable natural resource use and planning, for resilient landscapes in the face of changing socio-economic and environmental pressures. The LULC trends depicted by this study are comparable to other studies in similar dryland environments across Kenya and beyond. For instance Kirui and Mirzabaev [66], Omwoyo, et al. [60] and Musyoka and Onjala [67] reported similar possible drivers of LULC change in the drylands of East Africa, including population increase, infrastructural developments and expansion agricultural activities. Despite the use of medium satellite images providing critical information for decision making, future rstudies should focus on integrating higher-resolution satellite images and advanced modeling techniques to capture finer-scale changes and provide more accurate predictions of LULC dynamics in dryland ecosystems of Kenya.

5 Conclusion

The study conducted a comprehensive analysis of land use and land cover (LULC) dynamics in the Kibwezi West region from 1990 to 2051. LULC classification was performed using supervised classification, and the 2051 LULC map was predicted using the Random Forest algorithm. Six LULC classes were identified: Forested land, shrubland, grassland, cropland, water body and other lands. The overall classification accuracy of 78.04% and Kappa Coefficient of 0.61 were satisfactory for further LULC change analyses. Cropland, grassland and other lands experienced a net gain in coverage area, while forested land, shrubland and water body showed a net loss between 1990 to 2021. A projected net loss in coverage area for forested land, shrubland, water body and other lands was predicted for the period from 2021 to 2051.

These findings highlight significant transformations in LULC classes over the decades, offering insights into patterns of change and potential future trajectories. The results contribute to the body of knowledge on LULC dynamics, which will support evidence-based decision-making processes for sustainable land use planning, natural resource management and environmental conservation efforts in Kibwezi West and similar landscapes. Moving forward, there is a need for comprehensive and sustainable land resource management strategies in Kenya's drylands. Future policy interventions should promote sustainable agricultural practices, sustainable land use management and conservation of natural habitats to support the growing population while preserving ecological integrity.

Acknowledgements This work was conducted as part of PhD thesis research sponsored by the University of Nairobi.

Author contributions AMO conceptualised the study, conducted data analysis and wrote the main manuscript text. RNO conceptualised the study, reviewed the manuscript text. OVW reviewed the manuscript text. MJK reviewed the manuscript text.

Data availability Data will be shared on request.

Declarations

Competing interests The authors declare no competing interests.

References

1. Wang J, Bretz M, Dewan MAA, Delavar MA. Machine learning in modelling land-use and land cover-change (LULCC): current status, challenges and prospects. Sci Total Environ. 2022;822: 153559. https://doi.org/10.1016/j.scitotenv.2022.153559.
2. Ellis EC. Land use and ecological change: a 12,000-year history. Annu Rev Environ Resour. 2021;46:1–33. https://doi.org/10.1146/annurev-environ-012220-010822.
3. Long H, Zhang Y, Ma L, Tu S. Land use transitions: progress, challenges and prospects. Land. 2021;10(9):903. https://doi.org/10.3390/land10090903.
4. Hertel TW, West TA, Börner J, Villoria NB. A review of global-local-global linkages in economic land-use/cover change models. Environ Res Lett. 2019;14(5): 053003. https://doi.org/10.1088/1748-9326/ab0d33.
5. Dorninger C, et al. The effect of industrialization and globalization on domestic land-use: a global resource footprint perspective. Glob Environ Chang. 2021;69: 102311. https://doi.org/10.1016/j.gloenvcha.2021.102311.
6. Norton GW, Alwang J, Masters WA. Economics of agricultural development: world food systems and resource use. Amsterdam: Routledge; 2021.
7. Pereira JD. Colonialism and customary land tenure in africa: portuguese representations and policies during the 19th and 20th centuries. Afr Stud. 2024. https://doi.org/10.1080/00020184.2024.2307553.
8. Achiba GA, Lengoiboni MN. Devolution and the politics of communal tenure reform in Kenya. Afr Aff. 2020;119(476):338–69. https://doi.org/10.1093/afraf/adaa010.
9. Mganga K, Musimba N, Nyariki D, Nyangito M, Mwang'ombe AW. The choice of grass species to combat desertification in semi-arid Kenyan rangelands is greatly influenced by their forage value for livestock. Grass Forage Sci. 2015;70(1):161–7. https://doi.org/10.1111/gfs.12089.

10. Zowe MK, Musimba N, Nyariki D, Nyariki D. Combining sustainable land management technologies to combat land degradation and improve rural livelihoods in semi-arid lands in Kenya. Environ Manage. 2015;56(6):1538–48. https://doi.org/10.1007/s00267-015-0579-9.
11. Kinyili BM. The nexus of climate change and land-use in Kenya. Int J Environ Climate Change. 2023;13(8):2228–41. https://doi.org/10.9734/ijecc/2023/v13i82181.
12. Njue PN, Musyimi M. Building information modelling in urbanising Kenya. Int J Eng Manage Res. 2023;13(1):136–43. https://doi.org/10.31033/ijemr.13.1.18.
13. Roy PS, et al. Anthropogenic land use and land cover changes—A review on its environmental consequences and climate change. J Indian Soc Remote Sens. 2022;50(8):1615–40. https://doi.org/10.1007/s12524-022-01569-w.
14. Idoumskine I, Aydda A, Ezaidi A, Ramouch K, Haddou MA. Assessing impact of land use/land cover dynamic on urban climate change in a semi-arid region-case study of Agadir City (Morocco). Ecol Eng. 2024. https://doi.org/10.12912/27197050/183636.
15. Zhang Z, et al. Socio-economic impacts of agricultural land conversion: a meta-analysis. Land Use Policy. 2023;132: 106831. https://doi.org/10.1016/j.landusepol.2023.106831.
16. Ruttoh RC, Obiero JP, Omuto CT, Tanui L. Assessment of land cover and land use change dynamics in Kibwezi Watershed, Kenya. Sci World J. 2022. https://doi.org/10.1155/2022/3944810.
17. Assede ES, Orou H, Biaou SS, Geldenhuys CJ, Ahononga FC, Chirwa PW. Understanding drivers of land use and land cover change in Africa: a review. Curr Landscape Ecol Rep. 2023. https://doi.org/10.1007/s40823-023-00087-w.
18. Asenso Barnieh B, Jia L, Menenti M, Zhou J, Zeng Y. Mapping land use land cover transitions at different spatiotemporal scales in West Africa. Sustainability. 2020. https://doi.org/10.3390/su12208565.
19. Emongor R, Maina F, Nyongesa D, Ngoru B, Emongor V. Food and nutrition security and wildlife conservation: case studies from Kenya. Amsterdam: Elsevier; 2021.
20. Kiruki HM, van der Zanden EH, Gikuma-Njuru P, Verburg PH. The effect of charcoal production and other land uses on diversity, structure and regeneration of woodlands in a semi-arid area in Kenya. For Ecol Manage. 2017;391:282–95. https://doi.org/10.1016/j.foreco.2017.02.030.
21. Omwoyo AM, Onwonga RN, Wasonga VO, Mwangi JK. Influence of selected land use and land cover types on greenhouse gas fluxes in drylands of Eastern Kenya. Soil Advances. 2024;1: 100005. https://doi.org/10.1016/j.soilad.2024.100005.
22. Wambua BN, Kithiia SM. Effects of soil erosion on sediment dynamics, food security and rural poverty in Makueni District, eastern Kenya. Int J Appl. 2014;4:1.
23. Mugambi JM, Kagendo J, Kweyu M, Mbuvi MTE. Influence of community forest association activities on dryland resources management: case of Kibwezi forest in Kenya. Management. 2020. https://doi.org/10.11648/j.ijnrem.20200503.16.
24. Mganga K, Musimba N, Nyariki D. Combining sustainable land management technologies to combat land degradation and improve rural livelihoods in semi-arid lands in Kenya. Environ Manage. 2015;56(6):1538–48.
25. Li T, et al. Managing multiple stressors for sustainable livelihoods in dryland ecosystems: insights and entry points for resource management. Land Degrad Dev. 2024;35(3):968–84. https://doi.org/10.1002/ldr.4964.
26. Omasire AK, Kimondiu J, Kariuki P. Urban sprawl causes and impacts on agricultural land in Wote town area of Makueni county, Kenya. Int J Environ Agric Biotechnol. 2020. https://doi.org/10.22161/ijeab.53.15.
27. Bishaw B, et al. Farmers' strategies for adapting to and mitigating climate variability and change through agroforestry in Ethiopia and Kenya. Corvallis, Oregon: Oregon State University; 2013.
28. Mueke M, Maitho T, Mbwesa J. An assessment of socio-economic benefits accrued by farmers in donor funded community development projects in Kibwezi irrigation project, Kenya. Res Humanit Soc Sci. 2015;5(17):65–73.
29. W. G. Sombroek, H. Braun, and B. Exploratory soil map and agro-climatic zone map of Kenya, 1980, scale 1: 1,000,000. 1982.
30. Musembi DK, Cheruiyot H. A case for validation of indigenous knowledge in forecasting rainfall among the Kamba community of Makueni county, lower Eastern Kenya. J Meteorol. 2016. https://doi.org/10.20987/jmrs.4.08.2016.
31. Nzioka P, Kamau S, Mwanzia V. The influence of ridge-furrow tillage systems on two sorghum varieties with contrasting drought Tolerance in Kibwezi West Sub-County, Kenya. J Afr Interdisc Stud. 2022;6(11):257–75.
32. Mantel S, Dondeyne S, Deckers S. World reference base for soil resources (WRB). Amsterdam: Elsevier; 2023.
33. Kevin ZM, Nashon KM, Dickson MN, Moses MN, Wellington NE, William MM. Different land use types in the semi-arid rangelands of Kenya influence soil properties. J Soil Sci Environ Manag. 2011;2(11):370–4.
34. El Fellah S, Rziza M, El Haziti M. An efficient approach for filling gaps in Landsat 7 satellite images. IEEE Geosci Remote Sens Lett. 2016;14(1):62–6. https://doi.org/10.1109/LGRS.2016.2626138.
35. Kearney SP, Smukler SM. Determining greenhouse gas emissions and removals associated with land-use and land-cover change. In: Rosenstock TS, editor. Methods for Measuring Greenhouse Gas Balances and Evaluating Mitigation Options in Smallholder Agriculture. Cham: Springer International Publishing; 2016. p. 37–70.
36. R. Core Team. R: A language and environment for statistical computing. R Foundation for Statistical Computing: Vienna, Austria; 2021.
37. Gashaw T, Bantider A, Mahari A. Evaluations of land use/land cover changes and land degradation in Dera District, Ethiopia: GIS and remote sensing based analysis. Int J Sci Res Environ Sci. 2014. https://doi.org/10.12983/ijsres-2014-p0199-0208.
38. Duveiller G, et al. Local biophysical effects of land use and land cover change: towards an assessment tool for policy makers. Land Use Policy. 2020. https://doi.org/10.1016/j.landusepol.2019.104382.
39. Keenan RJ, Reams GA, Achard F, de Freitas JV, Grainger A, Lindquist E. Dynamics of global forest area: results from the FAO global forest resources assessment 2015. For Ecol Manage. 2015;352:9–20. https://doi.org/10.1016/j.foreco.2015.06.014.
40. Biau G, Scornet E. A random forest guided tour. TEST. 2016;25:197–227.
41. Belgiu M, Drăguţ L. Random forest in remote sensing: a review of applications and future directions. ISPRS J Photogramm Remote Sens. 2016;114:24–31. https://doi.org/10.1016/j.isprsjprs.2016.01.011.
42. Nelson SA, Khorram S. Image processing and data analysis with ERDAS IMAGINE®. United States: CRC Press; 2018.
43. Rwanga SS, Ndambuki JM. Accuracy assessment of land use/land cover classification using remote sensing and GIS. Int J Geosci. 2017;8(04):611. https://doi.org/10.4236/ijg.2017.84033.

44. T. Wilson, "A review of sub-regional population projection methods," Report to the office of economic and statistical research. Queensland centre for population research, school of geography, planning and environmental management, The University of Queensland, Brisbane, 2011.
45. Masud S, Ali Z, Haq M, Ghuri BM. Monitoring and predicting landuse/landcover change using an integrated markov chain & multilayer perceptron models: a case study of sahiwal tehsil. J GeoSpace Sci. 2016;2:43–59.
46. Hakim A, Baja S, Rampisela D, Arif S. Spatial dynamic prediction of landuse/landcover change (case study: tamalanrea sub-district, makassar city). IOP Conf Series:Earth Environ Sci. 2019. https://doi.org/10.1088/1755-1315/280/1/012023.
47. Al-Hameedi WMM, Chen J, Faichia C, Nath B, Al-Shaibah B, Al-Aizari A. Geospatial analysis of land use/cover change and land surface temperature for landscape risk pattern change evaluation of Baghdad City, Iraq, using CA–Markov and ANN models. Sustainability. 2022;14(14):8568. https://doi.org/10.3390/su14148568.
48. El-Tantawi AM, Bao A, Chang C, Liu Y. Monitoring and predicting land use/cover changes in the Aksu-Tarim River Basin, Xinjiang-China (1990–2030). Environ Monit Assess. 2019;191:1–18. https://doi.org/10.1007/s10661-019-7478-0.
49. Exavier R, Zeilhofer P. OpenLand: software for quantitative analysis and visualization of land use and cover change. R J. 2020. https://doi.org/10.32614/RJ-2021-021.
50. Leta MK, Demissie TA, Tränckner J. Modeling and prediction of land use land cover change dynamics based on land change modeler (Lcm) in nashe watershed, upper blue nile basin, Ethiopia. Sustainability. 2021;13(7):3740. https://doi.org/10.3390/su13073740.
51. Jat MK, Choudhary M, Saxena A. Application of geo-spatial techniques and cellular automata for modelling urban growth of a heterogeneous urban fringe. Egyp J Remote Sens Space Sci. 2017;20(2):223–41. https://doi.org/10.1016/j.ejrs.2017.02.002.
52. Nouri J, Gharagozlou A, Arjmandi R, Faryadi S, Adl M. Predicting urban land use changes using a CA–Markov model. Arab J Sci Eng. 2014;39:5565–73. https://doi.org/10.1007/s13369-014-1119-2.
53. W. O. Oduke, D. K. Musembi, and P. C. Kariuki, "Changes in cropland between 1986 and 2019 in Kitui central sub-county, Kitui county, Kenya," 2021.
54. Chapa F, Hariharan S, Hack J. A new approach to high-resolution urban land use classification using open access software and true color satellite images. Sustainability. 2019;11(19):5266.
55. Mishra VN, Rai PK, Kumar P, Prasad R. Evaluation of land use/land cover classification accuracy using multi-resolution remote sensing images. In Forum Geografic. 2016. https://doi.org/10.5775/fg.2016.137.i.
56. Güneralp B, Lwasa S, Masundire H, Parnell S, Seto KC. Urbanization in Africa: challenges and opportunities for conservation. Environ Res Lett. 2017;13(1): 015002.
57. Sang CC, Olago DO, Nyumba TO, Marchant R, Thorn JP. Assessing the underlying drivers of change over two decades of land use and land cover dynamics along the standard gauge railway corridor, Kenya. Sustainability. 2022;14(10):6158. https://doi.org/10.3390/su14106158.
58. Ministry of Forestry and Wildlife. Analysis of drivers and underlying causes of forest cover change in the various forest types of Kenya; 2013.
59. Mwaura F, Kiringe JW, Warinwa F, Wandera P. Estimation of the economic value for the consumptive water use ecosystem service benefits of the Chyulu Hills watershed, Kenya. Int J Agricu Forestry Fisheries. 2016;4(4):36–48.
60. Omwoyo AM, Muthama NJ, Opere A, Onwonga R. Simulating stream flow in response to climate change in the Upper Ewaso Ngiro Catchment, Kenya. J Climate. 2017. https://doi.org/10.20987/jccs.1.02.2017.
61. Tesfay F, Tadesse SA, Getahun YS, Lemma E, Gebremedhn AY. Evaluating the impact of land use land cover changes on the values of ecosystem services in the Chacha Watershed, Ethiopia's central highland. Environ Sustain Indic. 2023;18: 100256.
62. Zacharia M, Elias A, Jeremiah K, Simon M, Olang L. "Assessment of land cover changes in lake Olbolosat region of the central Kenyan highlands using Landsat satellite imagery aided by indigenous knowledge. J Biodivers Manage Forestry. 2013. https://doi.org/10.4172/2327-4417.1000107.
63. Bren d'Amour C, et al. Future urban land expansion and implications for global croplands. Proc Nat Acad Sci. 2017;114(34):8939–44.
64. Laurance WF, Sayer J, Cassman KG. Agricultural expansion and its impacts on tropical nature. Trends Ecol Evol. 2014;29(2):107–16.
65. Huang J, Yu H, Guan X, Wang G, Guo R. Accelerated dryland expansion under climate change. Nat Clim Chang. 2016;6(2):166–71.
66. O. Kirui and A. Mirzabaev, "Drivers of land degradation and adoption of multiple sustainable land management practices in Eastern Africa," 2015.
67. Musyoka PK, Onjala J. Livelihood diversification and household vulnerability to climate shocks in rural Kenya. Int J Econ Dev Res (IJEDR). 2023. https://doi.org/10.37385/ijedr.v4i1.785.